Neurobiology of Disease

# Protease-Resistant Human Prion Protein and Ferritin Are Cotransported across Caco-2 Epithelial Cells: Implications for Species Barrier in Prion Uptake from the Intestine

**Ravi Shankar Mishra,* Subhabrata Basu,* Yaping Gu, Xiu Luo, Wen-Quan Zou, Richa Mishra, Ruliang Li, Shu G. Chen, Pierluigi Gambetti, Hisashi Fujioka, and Neena Singh**

Institute of Pathology, Case Western Reserve University, Cleveland, Ohio 44106

**Foodborne transmission of bovine spongiform encephalopathy (BSE) to humans as variant Creutzfeldt–Jakob disease (CJD) has affected over 100 individuals, and probably millions of others have been exposed to BSE-contaminated food substances. Despite these obvious public health concerns, surprisingly little is known about the mechanism by which PrP–scrapie ($PrP^{Sc}$), the most reliable surrogate marker of infection in BSE-contaminated food, crosses the human intestinal epithelial cell barrier. Here we show that digestive enzyme (DE) treatment of sporadic CJD brain homogenate generates a C-terminal fragment similar to the proteinase K-resistant $PrP^{Sc}$ core of 27–30 kDa implicated in prion disease transmission and pathogenesis. Notably, DE treatment results in a $PrP^{Sc}$–protein complex that is avidly transcytosed in vesicular structures across an *in vitro* model of the human intestinal epithelial cell barrier, regardless of the amount of endogenous $PrP^{C}$ expression. Unexpectedly, $PrP^{Sc}$ is cotransported with ferritin, a prominent component of the DE-treated $PrP^{Sc}$–protein complex. The transport of $PrP^{Sc}$–ferritin is sensitive to low temperature, brefeldin-A, and nocodazole treatment and is inhibited by excess free ferritin, implicating a receptor- or transporter-mediated pathway. Because ferritin shares considerable homology across species, these data suggest that $PrP^{Sc}$-associated proteins, in particular ferritin, may facilitate $PrP^{Sc}$ uptake in the intestine from distant species, leading to a carrier state in humans.**

*Key words:* **prion infection; subclinical infection; PrP transport; new variant CJD; ferritin; epithelial cell barrier; Caco-2**

## Introduction

The transmission of sheep scrapie to cattle as bovine spongiform encephalopathy (BSE) and its onward transmission to humans as variant Creutzfeldt–Jakob disease (vCJD) attests to the remarkably persistent and permeable nature of prions or PrP–scrapie ($PrP^{Sc}$) across species barriers (Hill et al., 1998; Collinge, 1999; Taylor, 2002). The BSE epidemic is far from over despite the concerted efforts of national, industrial, and regulatory agencies across the world. An emerging threat is the continual spread of chronic wasting disease in the deer and elk population in the United States and the uncertainties regarding its transmission to livestock and humans (Miller and Williams, 2003). As the sources of $PrP^{Sc}$-contaminated food products continue to increase, it has become increasingly critical to understand the mechanism by which $PrP^{Sc}$, a protein with a protease-resistant core of 27–30 kDa and a major, if not the only, component of prion infectivity (Prusiner, 1998), maneuvers its way across the impermeable and highly selective epithelial barrier of the human intestinal tract.

Retrospective examination of vCJD patients and animal models challenged orally with BSE-infected tissue show accumulation of $PrP^{Sc}$ in the Peyer's patches, lymphoid tissue lining the gastrointestinal (GI) tract, and peripheral and enteric nervous systems (Bons et al., 1999; Beekes and McBride, 2000; Foster et al., 2001; McBride et al., 2001; Nicotera, 2001; Haik et al., 2003; Aguzzi and Polymenidou, 2004). Uptake of $PrP^{Sc}$ from the lumen of the intestine is thought to be mediated by intestinal dendritic cells and M-cells lining the mucosa, after which it undergoes replication in the gut-associated lymphoid tissue. Subsequent transport to the CNS probably occurs along peripheral nerves (Heppner et al., 2001; Huang et al., 2002; Aguzzi and Polymenidou, 2004). However, a recent report demonstrating the absence of prion infectivity in $\mu$MT and RAG1$^{-/-}$ mice orally challenged with prions despite the presence of M-cells suggests that $PrP^{Sc}$ transport across the intestinal epithelial barrier is not limited to M-cells and that additional pathways must exist (Prinz et al., 2003).

Thus, to fully understand the mechanism of $PrP^{Sc}$ uptake from contaminated food by the intestinal epithelial cells, we investigated the transport of human $PrP^{Sc}$ from sporadic CJD brain tissue (sCJD–$PrP^{Sc}$) across a monolayer of Caco-2 cells with tight junctions, representing an *in vitro* model of the human intestinal epithelial cell barrier (Pinto et al., 1983). Here we show that pre-

Received July 15, 2004; revised Oct. 27, 2004; accepted Nov. 2, 2004.

This work was supported by National Institutes of Health Grants NS39089 and NS44209 to N.S. Normal and sporadic Creutzfeldt-Jakob disease human brain tissue was obtained from the National Prion Disease Surveillance Center and processed in the biosafety level 3 facility (supported by grants from the Centers for Disease Control and Prevention to P.G.). Technical assistance for the processing of electron microscopic sections was provided by Kiet-Dan Luc.

*R.S.M. and S.B. contributed equally to this work.

Correspondence should be addressed to Dr. Neena Singh, Institute of Pathology, Case Western Reserve University, 2085 Adelbert Road, Cleveland, OH 44106. E-mail: neena.singh@case.edu.

DOI:10.1523/JNEUROSCI.2864-04.2004

 0270-6474/04/2411280-11$15.00/0

treatment of sCJD brain homogenate with digestive enzymes (DEs), in particular stomach pepsin, generates a protease-resistant C-terminal fragment similar to the proteinase K (PK)-resistant core of $PrP^{Sc}$ (PrP27–30) implicated in the transmission and pathogenesis of prion disorders (Prusiner, 1998). Unexpectedly, both PK and DE treatments generate a $PrP^{Sc}$–protein complex that includes ferritin as a major component, and the $PrP^{Sc}$–ferritin complex is cotransported across Caco-2 cells in vesicular structures. The transport of $PrP^{Sc}$–ferritin complex is inhibited by excess free ferritin, low temperature, and by treatment with brefeldin-A or nocodazole, implicating a receptor- or transporter-mediated transcytotic path across Caco-2 cells. These data provide insight into the cellular mechanisms by which $PrP^{Sc}$ ingested with contaminated food crosses the intestinal epithelium and the possibility of devising practical methods for blocking its uptake.

## Materials and Methods

*Materials and chemicals.* Normal human brain tissue was obtained from frozen samples from a 61-year-old female and diseased tissue from a 66-year-old male with a confirmed diagnosis of sCJD. Human colon carcinoma cell lines Caco-2 (C2BBe1) (Peterson et al., 1992) and HT-29 were obtained from American Type Culture Collection (Manassas, VA). The following anti-PrP antibodies were used in this study: 3F4 (residues 109 and 112; Signet Laboratories, Dedham, MA), 8H4 (residues 175–185; obtained from our facility), 8B4 (residues 37–44; obtained from our facility), and 6H4 (residues 144–152; Prionics). The antibody against the tight junction protein zonula occludens-1 (ZO-1) was purchased from Zymed (San Francisco, CA). Polyclonal anti-ferritin antibody was obtained from Sigma (St. Louis, MO). RITC- and FITC-labeled secondary antibodies were obtained from Southern Biotechnology (Birmingham, AL). Sulfo-NHS-biotin and streptavidin–Texas Red were obtained from Pierce (Rockford, IL). Cell culture supplies were obtained from Invitrogen (Carlsbad, CA). Pure human liver and spleen ferritin and all other chemicals were obtained from Sigma.

*Cell culture and preparation of epithelial cell monolayers.* Caco-2 cells were cultured in DMEM supplemented with 10% fetal bovine serum in a 10% $CO_2$ atmosphere and passaged weekly. For preparing monolayers, cells from a confluent flask were resuspended in DMEM at a concentration of $2 \times 10^8$ cells/ml and added to the apical (AP) chamber of polycarbonate filters [Transwell; 12 or 24 mm diameter (1 and 4.7 $cm^2$, respectively); 3 $\mu$m pore size; Costar, Cambridge, MA]. The filters were placed in a 12- or 6-well culture dish containing 0.6 or 1.2 ml of DMEM, respectively. The medium was replaced every day until confluent monolayers with tight junctions developed (10–14 d). The integrity of tight junctions was monitored by measuring transepithelial electrical resistance (TEER) across the monolayer with a millicell-ERS instrument (Millipore, Bedford, MA) and by measuring the transfer of $^3$H-inulin from the AP to the basolateral (BL) chamber. Monolayers exhibiting a TEER of $>400\ \Omega/cm^2$ and a $^3$H-inulin transport of $<0.01\%/cm^2$/min after 1 hr of incubation at 37°C were used for transport studies. For some studies, M17 cells cultured on polylysine-coated glass coverslips were placed in the BL chamber for the duration of the experiment.

*Transfection of Caco-2 cells.* The coding sequence of human PrP was subcloned into the eukaryotic expression vector cep4$\beta$ using the *Not*I and *Bam*HI restriction sites as described previously (Petersen et al., 1996) and transfected into Caco-2 cells with LipofectAMINE according to the manufacturer's (Invitrogen, Grand Island, NY) specifications. Transfected cells were selected and maintained in selective medium (500 $\mu$g/ml hygromycin) at 37°C in a humidified atmosphere supplemented with 10% $CO_2$.

*Preparation of DE- and PK-treated brain homogenates and immunoprecipitation.* For sample preparation, 0.1 gm of brain tissue from the frontal cortex was sonicated in 1 ml of PBS to obtain a 10% homogenate. Treatment with DEs was performed as described by Glahn et al. (1998). In short, 0.5 ml of 10% normal homogenate (NH) or sCJD homogenate (CJDH) in PBS was treated with 200 U of salivary amylase at 37°C for 15 min. The pH of the solution was adjusted to 2.0 with 5.0 M HCl, and 0.05 ml of pepsin (4095 U) was added. After additional rocking at 37°C for 1 hr, the pH was raised to 6.0 with 1 M sodium bicarbonate, and 0.2 ml of pancreatin–bile extract was added (0.00185 gm of pancreatin and 0.011 gm of bile extract/ml of 0.1 M $NaHCO_3$). The pH was raised to 7.4 with 6N sodium hydroxide, and 0.0084 ml each of 2 M NaCl and KCl solutions was added. The mixture was again rocked at 37°C for 2 hr. At the end of the digestion, the added enzymes were inactivated with 4 mM PMSF and a mixture of protease inhibitors containing 10 $\mu$g/ml each of leupeptin, antipain, and pepstatin, and the digest was stored at −70°C for additional use. The same mixture of protease inhibitors was used throughout this study.

For PK treatment, the homogenate was supplemented with lysis buffer (1% NP-40, 0.5% sodium deoxycholate, 100 mM NaCl, and 10 mM EDTA in 20 mM Tris-HCl, pH 7.4) and treated with 50 $\mu$g/ml PK at 37°C for 1 hr. The reaction was terminated with 4 mM PMSF and a mixture of protease inhibitors (described above), and the homogenate was frozen at −70°C for additional use.

For immunoprecipitation, untreated or PK- or DE-treated NHs and sCJDHs were centrifuged at $3000 \times g$ for 15 min at 4°C, and the supernatant was subjected to immunoprecipitation with either anti-ferritin or anti-PrP antibodies 6H4 or 8H4, as described previously (Mishra et al., 2002). The protein complexes were eluted from protein A beads with low pH glycine buffer, the pH was adjusted, and small aliquots of immunoprecipitated samples were frozen for additional use. Transport studies were performed in duplicate with each of these samples simultaneously to minimize experimental error.

*Purification of $PrP^{Sc}$ from sCJD brain homogenate.* For the isolation of purified $PrP^{Sc}$, 0.3 gm of sCJD brain sample was homogenized in PBS to yield a 10% homogenate and biotinylated with 1 mg/ml sulfo-NHS-biotin (Pierce) overnight at 4°C. Excess biotin was quenched with 50 mM glycine and by washing three times with PBS in a centricon with a 3 kDa cutoff. Biotinylated CJDH was supplemented with an equal volume of 2× lysis buffer and centrifuged at $890 \times g$ for 10 min to pellet large aggregates (P1). The recovered supernatant (S1) was ultracentrifuged at $100{,}000 \times g$ for 1 hr at 4°C to obtain the pellet P2, which was resuspended again in lysis buffer and recentrifuged to obtain the pellet P3. At this stage, the pellet was redissolved in TNSS buffer (10 mM Tris, 1 mM EDTA, 1 mM DTT, 1% sarcosyl, and 135 mM NaCl) and treated with 50 $\mu$g/ml PK at 37°C for 1 hr. The reaction was stopped with 4 mM PMSF and the mixture of protease inhibitors and subjected to an additional round of ultracentrifugation at $200{,}000 \times g$ for 2 hr to obtain the $PrP^{Sc}$-rich pellet fraction P4. The pellet P4 was resuspended again in TNSS buffer and recentrifuged at the same speed to obtain sequentially pellet fractions P5 and P6. In parallel, normal brain tissue was subjected to a similar treatment and used as a control for transport and binding experiments. The pellet P6 obtained from both sCJD and normal brain tissue was resuspended in 100 $\mu$l of PBS and sonicated with an equal volume of 20% purified human brain total lipid extract obtained from Avanti Polar Lipids (Alabaster, AL) to yield a 10% lipid–protein mixture. The resulting $NH^{Pellet}$– and $CJDH^{Pellet}$–brain lipid suspensions were diluted in PBS containing 1% BSA and used for binding and competition experiments.

*Measurement of $PrP^{Sc}$ transport.* In a typical experiment, monolayers of Caco-2 cells were washed with serum-free medium, and 20 $\mu$l of sample dissolved in 1 ml of serum-free medium was added to the AP chamber. The sample consisted of NH or CJDH that was untreated, PK or DE treated, or DE treated and mixed with 10 $\mu$M PrP peptide 106–126. The inserts were placed in a 6-well dish containing 1.2 ml of serum-free medium and incubated overnight at 37°C. Subsequently, AP and BL media samples were collected and centrifuged to pellet cell debris, and proteins from the supernatant were isolated by cold methanol precipitation. For preparation of cell lysate, cells on monolayers were treated with lysis buffer, and proteins were precipitated as above. All samples were boiled in sample buffer, resolved by SDS-PAGE, electroblotted to a polyvinylidene difluoride (PVDF) membrane, and probed with specific antibodies.

Quantitative analysis was performed by measuring the total raw density of $PrP^{Sc}$ bands in the AP and BL medium from duplicate samples. Each experiment was repeated five to eight times, and the statistical significance was evaluated by Student's *t* test.

*Silver staining of total proteins.* After SDS-PAGE, proteins were stained with the silver staining kit according to the instructions provided by the manufacturer (Bio-Rad, Hercules, CA).

*Competitive inhibition experiments.* Caco-2 monolayers cultured on filter inserts were cut out with a sharp scalpel and inverted with the cell side down on 16 μl of $NH^{Pellet}$ or $CJDH^{Pellet}$ suspension mixed in 84 μl of PBS containing 1% BSA or 0, 0.5, 1.0, and 1.5 μg/ml human spleen or liver ferritin dissolved in the same buffer. After a 30 min incubation on ice, filters were removed and washed gently in ice-cold PBS. Subsequent incubation with the specified sample was performed similarly. The cells were then fixed with 4% paraformaldehyde, immunostained as such on filters, and mounted with the cell side facing the coverslip for confocal microscopy.

*Immunostaining and confocal microscopy.* Cells were cultured on poly-D-lysine-coated glass coverslips or on transparent Transwell filters. After a particular experimental treatment, cells were fixed and processed for staining or first permeabilized with Triton X-100 and reacted with one of the following primary antibodies: monoclonal anti-PrP 8H4 (1:20), polyclonal rabbit anti-ferritin (1:20), or polyclonal anti-ZO-1 (1:20), followed by RITC- or FITC-conjugated appropriate (mouse or rabbit) secondary antibodies as described previously (Gu et al., 2003a,b). Streptavidin–Texas Red was used at a concentration of 1:40. Immunostained cells were mounted in gel mount and observed using a laser-scanning confocal microscope (Bio-Rad MRC 600). Horizontal sections were imaged using a 60× objective, and a magnification of 1.0 or 2.5 at different depths beginning from the top of the cells until the filter pores were visible. Vertical images were captured similarly using one filter at a time (green or red). Selected samples were reexamined and imaged using the LSM 5105 confocal microscope (Zeiss, Oberkochen, Germany).

*Electron microscopy (transmission electron microscopy).* Caco-2 cells on filter inserts were exposed to 8H4-immunoprecipitated CJDH–$PrP^{Sc}$ for 2 hr and fixed in a buffer containing glutaraldehyde (2.5%), paraformaldehyde (2%), and sucrose (4%) in phosphate buffer (0.05 M, pH 7.4) for 2 hr. Cell monolayer on the filter was cut out of the inserts and postfixed with 1% osmium tetroxide for 1 hr, followed by 30 min of *en bloc* staining with 1% aqueous uranyl acetate. Cells were then dehydrated in ascending concentrations of ethanol and embedded in Epon 812. Ultrathin sections were treated with 1% periodic acid for 4 min and stained with 2% uranyl acetate and lead citrate in 50% methanol. Processing of the 8H4-immunoprecipitated material was similar, with the modification that the sample was fixed, osmicated and treated with uranyl acetate in solution, and embedded in agar by centrifugation on a 1.5% agar block in an Eppendorf tube. The Eppendorf tube was then cut open with a blade, and the pellet embedded in agar was dehydrated and processed as above. All samples were examined using a CEM902 electron microscope (Zeiss).

## Results

### Human sCJD–$PrP^{Sc}$ is partially proteolyzed by DEs

$PrP^{Sc}$ ingested with contaminated meat is exposed to the harsh environment within the GI tract before uptake by the lining epithelium. During this process, the effect of DE and variable pH on the structure and stability of $PrP^{C}$ and $PrP^{Sc}$ are not known. To address this question, samples of NH and CJDH were subjected to sequential treatment with DE to simulate the *in vivo* conditions. Beginning with amylase at pH 7.4, the homogenates were sequentially treated with pepsin at pH 2.0, followed by pancreatin and bile extract at pH 6.0.

The effect of DE on $PrP^{Sc}$ was compared with conventional PK treatment by subjecting mock-treated, PK-treated, and DE-treated samples to Western blot analysis with anti-PrP antibody 3F4. Mock-treated NH reveals the diglycosylated, monoglycosylated, and unglycosylated forms of $PrP^{C}$ migrating at 35–37, 28–30, and 27 kDa respectively (Fig. 1*A*, lane 1). Similar glycoforms are detected in mock-treated CJDH, although the ratio of the three glycoforms is altered (Fig. 1*A*, lane 4). Treatment with PK or DE results in complete proteolysis of $PrP^{C}$ in NH (Fig. 1*A*, lanes 2, 3), whereas CJDH samples show faster migrating forms of 27–30 and 19 kDa, consistent with the migration of infectious and pathogenic PK-resistant $PrP^{Sc}$ (Fig. 1*A*, lanes 5, 6). Although this outcome is expected after PK treatment of CJDH, the generation of similar glycoforms with DE is noteworthy, suggesting comparable cleavage of $PrP^{Sc}$ by the two procedures. Additional confirmation of DE-mediated cleavage of $PrP^{Sc}$ was obtained by reblotting PK- and DE-treated CJDH samples with antibodies specific to the N or C terminus of PrP. As expected, there was no immunoreaction with the N-terminal antibody 8B4 and strong reactivity with C-terminal antibody 8H4 (data not shown). Evaluation of sCJD brain homogenate after treatment with individual DEs revealed that the cleavage of $PrP^{Sc}$ is mediated by pepsin at pH 2.0 (data not shown).

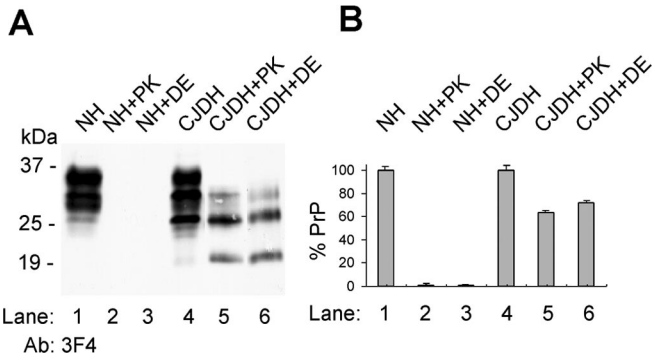


**Figure 1.** Human sCJD–$PrP^{Sc}$ is partially proteolyzed by DEs. *A*, Immunoblotting of NH and CJDH with 3F4 shows the three glycoforms of PrP migrating at 35–37, 28–30, and 27 kDa (lanes 1, 4). Treatment of NH with PK or DE results in almost complete digestion of $PrP^{C}$ (lanes 2, 3), whereas similar treatment of CJDH results in N-terminally truncated $PrP^{Sc}$ forms migrating at 19–30 kDa (lanes 5, 6). *B*, Densitometric analysis indicates hydrolysis of 97–98% of $PrP^{C}$ in NH by PK or DE, whereas $PrP^{Sc}$ in CJDH shows limited resistance to PK (68%) and DE (75%).

Quantitative estimation of the above results shows that 2 and 3% of PrP in NH samples and 68 and 75% of PrP in CJDH samples resist PK and DE treatment, respectively (Fig. 1*B*). Thus, by the time ingested $PrP^{Sc}$-contaminated meat reaches the intestine, almost all of $PrP^{C}$ is proteolyzed, and $PrP^{Sc}$ is converted to the protease-resistant C-terminal core of 27–30 kDa.

### DE-treated sCJD–$PrP^{Sc}$ is transported across Caco-2 epithelial cells

The transport of $PrP^{C}$ and $PrP^{Sc}$ in NH and CJDH across intestinal epithelial cells was assessed in an *in vitro* model comprising Caco-2 cell monolayers with tight junctions (Pinto et al., 1983). For all experiments, Caco-2 monolayers exhibiting a TEER of $>400\ \Omega/cm^2$ and $^3$H-inulin transport from the AP chamber to the BL chamber of $<0.01\%/cm^2$/min were used. Transport of $^3$H-inulin was compared before and after each treatment to rule out any toxic effects of the homogenate or $PrP^{Sc}$ during the experiment. Each sample was tested in duplicate, and each experiment was repeated at least five times.

In a typical experiment, 20 μl of NH or CJDH that had been mock treated, PK treated, DE treated, or DE treated and mixed with the PrP peptide 106–126 (10 μM) was added to the AP chamber of Caco-2 monolayers in serum-free medium and incubated overnight at 37°C. Subsequently, medium was collected from the AP and BL chambers, and methanol-precipitated proteins from the media and cell lysate samples were fractionated by SDS-PAGE, transblotted to a PVDF membrane, and probed with 3F4. In the NH sample, practically all of the added PrP is recovered from the AP medium, indicating negligible transport to the BL chamber (Fig. 2*A*, lanes 1–3). As expected, NH-PK and NH-DE samples show barely detectable PrP signal in the AP or

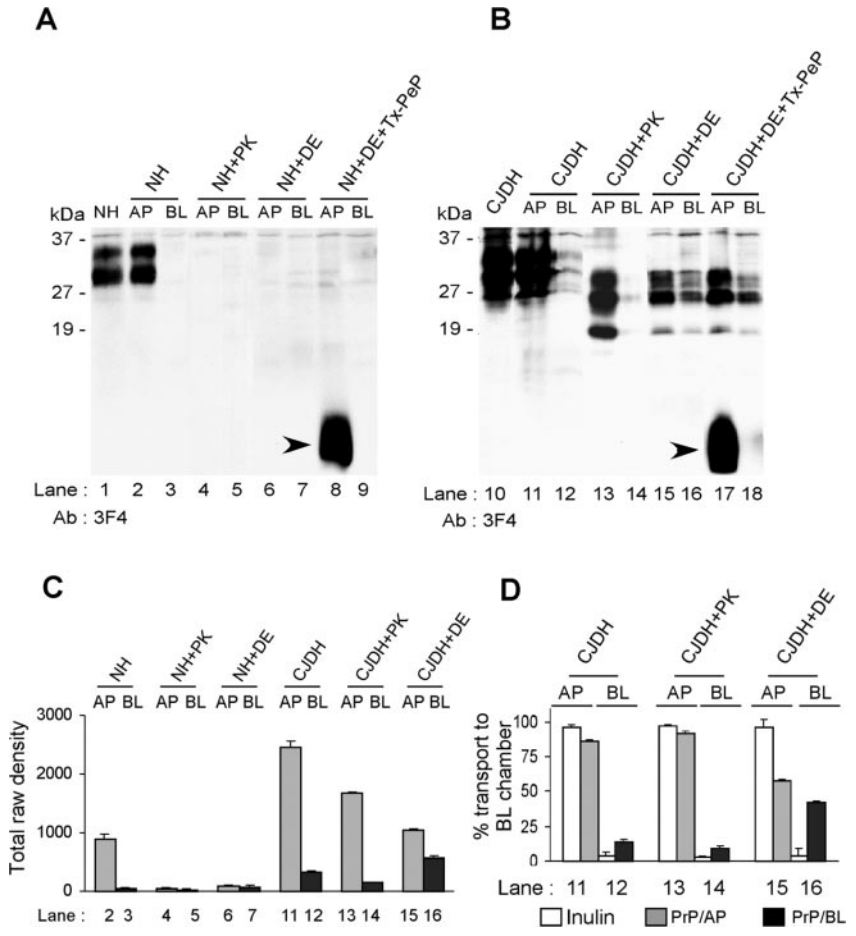


**Figure 2.** DE-treated sCJD–PrP$^{Sc}$ is transported across Caco-2 epithelial cells. An aliquot of mock-treated, PK-treated, or DE-treated NH or CJDH was added to the AP chamber of Caco-2 monolayers, and PrP transported to the BL chamber was estimated after an overnight incubation. *A*, Immunoblotting of proteins from the AP and BL media with 3F4 shows no detectable PrP signal in the BL chamber of cells exposed to mock-treated (lanes 2, 3), PK-treated (lanes 4, 5), or DE-treated (lanes 6–9) NH. *B*, In contrast, a significant PrP signal is detected in the BL chamber of cells exposed to mock-treated (lanes 11, 12), PK-treated (lanes 13, 14), or DE-treated (lanes 15–18) CJDH. PrP peptide 106–126 (Tx-pep) is not transported to the BL chamber when mixed with either DE-treated NH (*A*; lanes 8, 9, arrowhead) or DE-treated CJDH (*B*; lanes 17, 18, arrowhead). Lanes 1 and 10 show PrP reactivity in the starting NH and CJDH samples, respectively. *C*, Measurement of total raw density of PrP signal indicates minimal transport of PrP from mock-treated NH. In PK-treated and DE-treated NH samples, as expected, minimal PrP signal is detected. In contrast, a prominent PrP signal is detected in the AP and BL chambers of monolayers exposed to similarly treated CJDH samples (lane numbers correspond to samples in *A* and *B*). *D*, Quantitative estimation shows transport of 14, 8.5, and 42% of PrP from the AP chamber to the BL chamber from mock-treated, PK-treated, and DE-treated CJDH, respectively. Transport of $^3$H-inulin was $<0.01\%/cm^2$/min before and after the completion of each experiment. The error bar represents the mean ± SD of four experiments. $p < 0.01$.

BL samples (Fig. 2*A*, lanes 4–7). However, PrP106–126 (toxic peptide) is easily detected in the AP medium of NH-DE plus toxic peptide sample, ruling out experimental error in the detection of any leftover PrP (Fig. 2*A*, lane 8, arrowhead). In contrast, PrP in CJDH and protease-resistant PrP$^{Sc}$ in PK- and DE-treated CJDH samples are transported to the BL chamber (Fig. 2*B*, lanes 10–16). Surprisingly, PrP$^{Sc}$ in DE-treated CJDH is transported more efficiently than from the PK-treated sample (Fig. 2*B*, lanes 13–18). The PrP106–126 peptide mixed with CJDH-DE is not transported, although a bold PrP$^{Sc}$ signal is detected in the BL chamber of CJDH-DE plus toxic peptide sample (Fig. 2*B*, lanes 17, 18, arrowhead). No PrP signal was detected in any of the Caco-2 lysate samples (data not shown).

Quantification of the PrP signal in the AP and BL chambers of monolayers exposed to NH or CJDH and the percentage of transport of PrP in CJDH from the AP to the BL chamber are shown in Figure 2, *C* and *D*, respectively. In the mock-treated NH sample, almost all PrP is recovered from the AP chamber, with insignificant transport to the BL chamber (Fig. 2*C*, lanes 2, 3). In the PK- and DE-treated NH samples, as expected, barely any PrP is detected in the AP or BL chambers (Fig. 2*C*, lanes 4–7). In contrast, a significant proportion of PrP$^{Sc}$ from the CJDH samples is transported from the AP to the BL chambers (Fig. 2*C*, lanes 11–16), representing a transport of 14, 8.5, and 42% of PrP$^{Sc}$ from mock-treated, PK-treated, and DE-treated CJDH, respectively (Fig. 2*D*, lanes 11–16). The transport of $^3$H-inulin across the same monolayer is $<0.01\%/cm^2$/min in 1 hr at 37°C (Fig. 2*D*), confirming the integrity of tight junctions under these experimental conditions.

### Overexpression of PrP$^C$ does not alter the transport of sCJD–PrP$^{Sc}$ across Caco-2 cells

To evaluate whether the level of PrP$^C$ expression on Caco-2 cells influences PrP$^{Sc}$ uptake or transport, Caco-2 cells were transfected with a plasmid encoding human PrP$^C$, and the percentage of increase in PrP$^C$ expression was estimated. Immunoblotting of cell lysates prepared from human neuroblastoma, nontransfected Caco-2, and PrP$^C$-transfected Caco-2 (Caco-2$^{PrP}$) cells with 3F4 shows a 2.5-fold increase in PrP$^C$ expression by Caco-2$^{PrP}$ cells compared with nontransfected Caco-2 cells and 1.25 times that of M17 neuroblastoma cells (Fig. 3*A*, lanes 1–3, *B*).

The influence of increased PrP$^C$ expression on PrP$^{Sc}$ transport was estimated by isolating a crude fraction of PrP$^{Sc}$ from PK-treated CJDH to avoid the influence of membrane in mediating PrP$^{Sc}$ transport (Baron and Caughey, 2003). Accordingly, 20 $\mu$l of PK-treated CJDH was methanol precipitated, and the pellet was resuspended in PBS and added to the AP chamber of Caco-2 and Caco-2$^{PrP}$ monolayers. After an overnight incubation, AP and BL media were analyzed by immunoblotting and densitometric analysis as above. No significant difference is observed in the amount of PrP$^{Sc}$ transported across Caco-2$^{PrP}$ compared with nontransfected Caco-2 cells (Fig. 3*C*, lanes 1–4, *D*). These results were further confirmed by comparing the transport of PrP$^{Sc}$ across HT-29 cells, another human intestinal epithelial cell line that expresses twofold more PrP$^C$ than Caco-2. No significant difference was observed in the rate or quantity of PrP$^{Sc}$ transported across Caco-2 and HT-29 cells (data not shown), suggesting that the host PrP$^C$ expression level does not influence the internalization of PrP$^{Sc}$ by epithelial cells.

### Protease-resistant human sCJD–PrP$^{Sc}$ is associated with ferritin

We next attempted to purify PrP$^{Sc}$ from sCJDH to determine the impact of other molecules or proteins on its transport across

Caco-2 cells. Thus, sCJDH was subjected to PK treatment and repeated rounds of ultracentrifugation as described in Materials and Methods. The clarified supernatant from CJDH (S1), the supernatant and pellet fractions after the first round of ultracentrifugation (S2 and P2, respectively), and four subsequent rounds of ultracentrifugation (S3–S6 and P3–P6) were precipitated with cold methanol, fractionated by SDS-PAGE, and transblotted. Probing with 3F4 reveals PK-resistant glycoforms of $PrP^{Sc}$ representing the N-terminal truncated diglycosylated, monoglycosylated, and unglycosylated forms migrating at 29 and 30, 22–25, and 19 kDa, respectively, in the S1 fraction (Fig. 4*A*, lane 1). After the first round of ultracentrifugation, ~40% of $PrP^{Sc}$ fractionates in the supernatant fraction (S2), and ~60% is detected in the pellet (P2) (Fig. 4*A*, lanes 2, 3). In subsequent rounds, all of the $PrP^{Sc}$ is detected in the pellet fractions (P3–P6) (Fig. 4*A*, lanes 5, 7, 9, 11).

To assess the purity of $PrP^{Sc}$ recovered in the P6 fraction, the sample was deglycosylated with PNGase-F, fractionated by SDS-PAGE, and visualized by silver staining. In the untreated sample, bands corresponding to the diglycosylated, monoglycosylated, and unglycosylated forms of $PrP^{Sc}$ are identified as in Figure 4*A* (Fig. 4*B*, lane 1). In addition, a prominent band migrating at 20 kDa is seen (Fig. 4*B*, lane 1). After deglycosylation, $PrP^{Sc}$ glycoforms collapse to 19 kDa (Fig. 4*B*, lane 2, arrowhead), whereas the 20 kDa band remains unchanged (Fig. 4*B*, lane 2, arrow). The band marked with an asterisk represents the added PNGase (Fig. 4*B*, lane 2). Sequencing of the 20 kDa band confirmed its identity as a mixture of heavy (H) and light (L) chains of ferritin. Additional verification was obtained by reprobing the membrane in Figure 4*A* with anti-ferritin antibody. Strong immunoreaction is detected with the 20 kDa band, confirming its identity as ferritin (Fig. 4*C*, lanes 1–11). It is remarkable that ferritin resists PK treatment and persistently pellets with $PrP^{Sc}$.

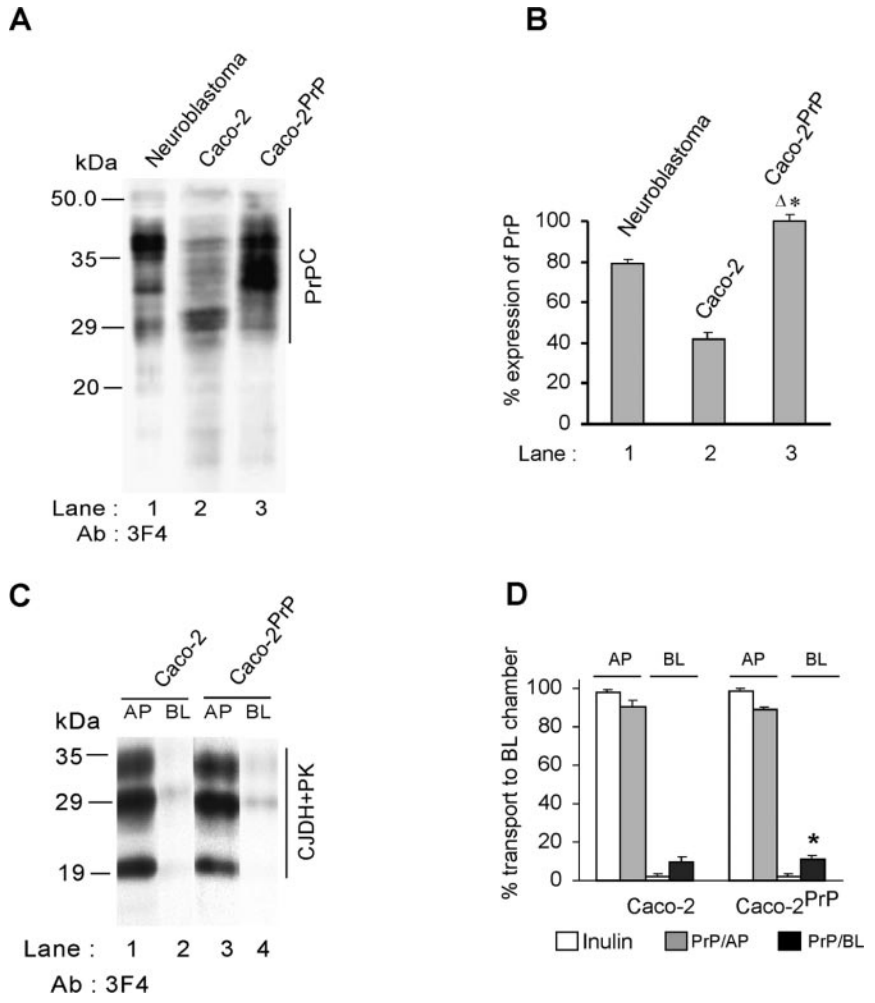


**Figure 3.** Overexpression of $PrP^{C}$ does not influence the transport of sCJD–$PrP^{Sc}$ across Caco-2 monolayers. Lysates of M17 neuroblastoma cells, Caco-2 cells, and transfected Caco-2$^{PrP}$ cells were immunoblotted with 3F4 to assess the level of PrP expression. *A*, Transfected Caco-2$^{PrP}$ expresses significantly more PrP compared with M17 and nontransfected Caco-2 cells (lane 3 vs lanes 1, 2). *B*, Quantitative estimation shows 2.5- and 1.5-fold PrP expression in Caco-2$^{PrP}$ cells compared with nontransfected Caco-2 and M17 cells, respectively [lane 3 vs lanes 1 ($^{*}p < 0.05$; $n = 3$) and lane 3 vs lane 2 ($^{\Delta}p < 0.01$; $n = 3$)]. *C*, Transport of PK-resistant $PrP^{Sc}$ across Caco-2 and Caco-2$^{PrP}$ cell monolayers was measured as in Figure 2. There is no significant difference in the amount of $PrP^{Sc}$ transported to the BL chamber of Caco-2$^{PrP}$ cells compared with nontransfected Caco-2 cells (lanes 3, 4 vs lanes 1, 2). *D*, Quantitative estimation shows transport of 10 and 11.2% of $PrP^{Sc}$ to the BL chamber of Caco-2 and Caco-2$^{PrP}$ cell monolayers, respectively. Each bar represents the mean ± SD of three experiments. $^{*}p < 0.05$.

The above results argue that either $PrP^{Sc}$ and ferritin happen to cosediment or the two proteins form a complex with each other, perhaps through ionic or hydrophobic interactions. To distinguish between these possibilities, the P6 pellet fraction was treated with NaCl varying in concentration from 0.1 to 1.0 M, and ferritin was eluted using DEAE-cellulose chromatography. Immunoblotting of the eluted fractions with 3F4 and anti-ferritin antibody shows complete elution of ferritin at 0.4 M NaCl (Fig. 4*D*, bottom, lanes 1–6). Almost all of the $PrP^{Sc}$ is retained in the column and is barely detected in the eluate (Fig. 4*D*, top, lanes 1–6).

Thus, $PrP^{Sc}$ and ferritin in the sCJD brain homogenate form a complex that is resistant to dissociation with low concentrations of salt. Whether this interaction occurs in the brain *in vivo* or after homogenization of brain tissue is unclear from our data.

Because it is unlikely that an aggregated and insoluble $PrP^{Sc}$–ferritin complex would be transported across the epithelial cell barrier, we focused our additional studies on the PK-resistant but detergent-soluble species of $PrP^{Sc}$ that is known to be infectious and can be immunoprecipitated with anti-PrP antibodies 8H4 and 6H4 (Safar et al., 1998; Paramithiotis et al., 2003; Pan et al., 2001). To determine whether protease-resistant, detergent-soluble $PrP^{Sc}$ is similarly associated with ferritin, mock-treated and DE-treated NH and CJDH were clarified by centrifugation at 3000 × *g* and subjected to immunoprecipitation with either anti-ferritin or anti-PrP antibody 8H4. Immune complexes were collected with protein A beads and washed, and eluted proteins were analyzed by immunoblotting with 3F4 or anti-ferritin antibodies. In samples immunoprecipitated with anti-ferritin and probed with 3F4, minimal PrP signal is detected in NH and NH-DE samples (Fig. 5*A*, lanes 1, 2). In contrast, surprisingly large

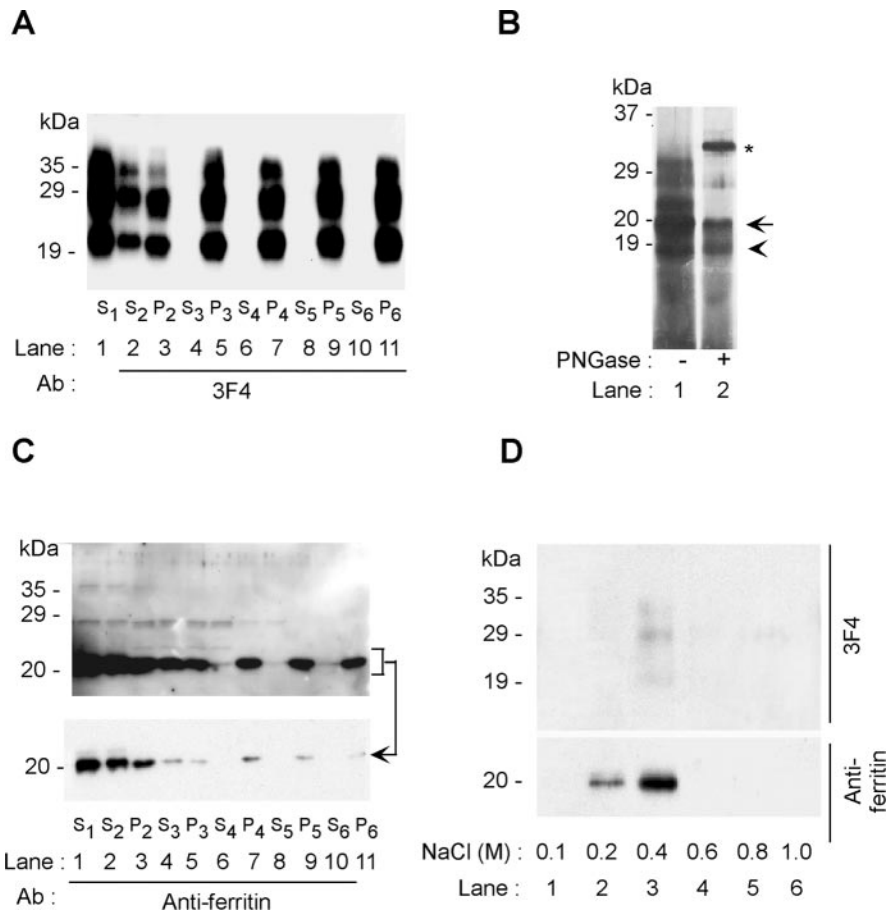


**Figure 4.** Protease-resistant sCJD–PrP$^{Sc}$ is associated with ferritin. Clarified supernatant obtained from PK-treated CJDH (S1) was subjected to five additional rounds of ultracentrifugation, and the resulting detergent-soluble supernatant (S2–S6) and detergent-insoluble pellet (P2–P6) fractions were immunoblotted with 3F4. *A*, The starting material (S1) and the supernatant and pellet fractions obtained after ultracentrifugation (S2 and P2, respectively) show the N-terminally truncated PrP$^{Sc}$ glycoforms migrating at 29 and 30, 22–25, and 19 kDa, respectively (lanes 1–3). After the first round of ultracentrifugation, 60% of PrP$^{Sc}$ fractionates in the pellet fraction (lanes 2, 3). After subsequent rounds of ultracentrifugation, all of the PrP$^{Sc}$ is detected in the pellet fractions (lanes 4–11). *B*, Silver staining of the P6 fraction shows PrP$^{Sc}$ glycoforms of 19–30 kDa and a 20 kDa band (lane 1). After treatment with PNGase, all PrP$^{Sc}$ glycoforms migrate at 19 kDa, as expected (lane 2, arrowhead), whereas the 20 kDa band remains insensitive to deglycosylation (lane 2, arrow). The slower migrating band in lane 2 (*) is derived from the added PNGase. *C*, Reprobing of the membrane in *A* with anti-ferritin antibody shows strong immunoreaction with the 20 kDa band and minor species migrating at 25 and 30 kDa (lanes 1–11). The 20 kDa band is detected in the first three fractions (lanes 1–3) and in all subsequent pellet fractions (lanes 4–11). *D*, The P6 fraction from *A* was treated with NaCl and subjected to DEAE-cellulose chromatography. Immunoblotting of eluted proteins with 3F4 and anti-ferritin antibodies shows dissociation of ferritin from PrP$^{Sc}$ at concentrations of 0.2–0.4 M NaCl (lanes 2, 3).

amounts of 3F4-immunoreactive PrP$^{Sc}$ from CJDH-DE and a small amount from CJDH sample coimmunoprecipitates with anti-ferritin (Fig. 5*A*, lanes 3, 4). Reprobing of the same membrane with anti-ferritin reveals the H and L chains of ferritin migrating at 21 and 20 kDa, respectively (Fig. 5*A*, lanes 5–8). In the CJDH-DE sample, additional slower migrating bands that react strongly with anti-ferritin antibody are detected (Fig. 5*A*, lane 8). Their identity is not clear at present. Immunoprecipitation of CJDH-DE with 8H4, followed by probing with 3F4 or anti-ferritin antibodies, shows similar association of PrP$^{Sc}$ with ferritin (Fig. 5*A*, lanes 9, 10). The apparent difference in the amount of PrP$^{Sc}$ and ferritin that coimmunoprecipitate with anti-ferritin versus 8H4 is probably attributable to the nature of the specific antibodies (N. Morel et al., 2004). DE treatment partially hydrolyzes the H chain of ferritin, which comigrates with the L chain at 20 kDa (Fig. 5*A*, lane 5 vs 6, 7 vs 8).

Silver staining of anti-ferritin- and 8H4-immunoprecipitated proteins from DE-treated NH and CJDH shows bands comigrating with ferritin at 20 kDa and several unidentified proteins (Fig. 5*A*, lanes 11–14). No PrP was immunoprecipitated in the absence of primary antibody from either mock-treated or DE-treated NH or CJDH, confirming that PrP$^{Sc}$ does not bind nonspecifically to protein A beads (Fig. 5*B*).

### sCJD–PrP$^{Sc}$ is cotransported with ferritin across Caco-2 cells

To determine whether PrP$^{Sc}$ is transported across Caco-2 cells in association with ferritin, 20 μl of CJDH-DE in serum-free medium was added to the AP chamber of filter inserts containing Caco-2 cell monolayers and incubated for 2 hr at 37°C. At the end of the incubation, monolayers were cut into two pieces: one half was immunostained for PrP and ferritin, and the other half was immunostained for the tight junction protein ZO-1. Transport of PrP and ferritin was checked by capturing horizontal confocal images at different depths as depicted in Figure 6*A* and by taking vertical images.

Staining for PrP (green) and ferritin (red) at level I shows colocalization of PrP and ferritin (Fig. 6*B*, panels 1–3, arrows) and limited reactivity for PrP alone (Fig. 6*B*, panels 1, 3, arrowheads). Similar images captured at level II (at the level of the filter pores) also show colocalization of PrP (green) and ferritin (red) (Fig. 6*B*, panels 4–6, arrows). Immunostaining for the tight junction protein ZO-1 (green) reveals intact tight junctions throughout the Caco-2 monolayer (Fig. 6*B*, panel 7). A vertical image through the same cells shows colocalization of PrP (green) and ferritin (red) at the AP and BL membranes (levels I and II) (Fig. 6*B*, panels 8–10). Transport of both PrP$^{Sc}$ and ferritin was significantly inhibited by incubation at 18°C and by pretreatment of the cells for 2 hr with brefeldin-A (3.5 μM) or nocodazole (33 μM), implicating a transcytotic process (data not shown).

### sCJD–PrP$^{Sc}$ remains associated with ferritin after transcytosis

To evaluate whether the PrP$^{Sc}$–ferritin complex remains intact after transcytosis across Caco-2 cells, filter inserts containing Caco-2 cell monolayers were placed in a 12-well dish containing M17 neuroblastoma cells cultured on glass coverslips in the BL chamber (Fig. 6*A*, diagram). Subsequently, 20 μl of CJDH-DE or biotinylated CJDH-DE was added to the AP chamber. The biotinylated sample was used to distinguish added PrP and ferritin from endogenous proteins expressed by M17 cells. After an overnight incubation, transcytosed PrP$^{Sc}$ and ferritin that had been subsequently endocytosed by M17 cells in the BL chamber were detected by immunostaining (Fig. 7*A*). The presence of tight junctions in Caco-2 cell monolayers was confirmed by immuno-

staining for ZO-1 and by checking the transport of $^{3}$H-inulin before and after incubation with CJDH-DE.

Immunostaining of Caco-2 monolayers for ZO-1 shows uniform staining, confirming the presence of tight junctions during the course of the experiment (Fig. 7*A*, panels 1, 5). Coimmunostaining of M17 cells for PrP (green) and ferritin (red) shows colocalization at several spots, indicating that some of the $PrP^{Sc}$–ferritin complexes remain intact even after transcytosis across Caco-2 cells (Fig. 7*A*, panels 2–4). Coimmunostaining of M17 cells for PrP (green) and streptavidin (red) (Fig. 7*A*, panels 6–8) confirms that the PrP signal is derived from the transcytosed, biotinylated CJDH-DE added to the AP chamber.

Electron microscopic analysis of the $PrP^{Sc}$–ferritin complex immunoprecipitated with 8H4 (as in Fig. 5*A*, lanes 9, 13) shows fibrillar material decorated with ferritin aggregates (Fig. 7*B*, top inset, arrows). When added to a monolayer of Caco-2 cells, the $PrP^{Sc}$–ferritin complex is seen in small and large phagocytic vesicles enclosed by a single membrane with the fibrillar material intact within these vesicles (Fig. 7*B*, top). Groups of these vesicles are subsequently transported out from the BL membrane and are seen within the pore of the Transwell membrane (Fig. 7*B*, bottom).

Together, the above data demonstrate that the $PrP^{Sc}$–ferritin complex is endocytosed together by Caco-2 cells and a significant proportion is transcytosed intact to the BL chamber, where it is endocytosed again by M17 cells.

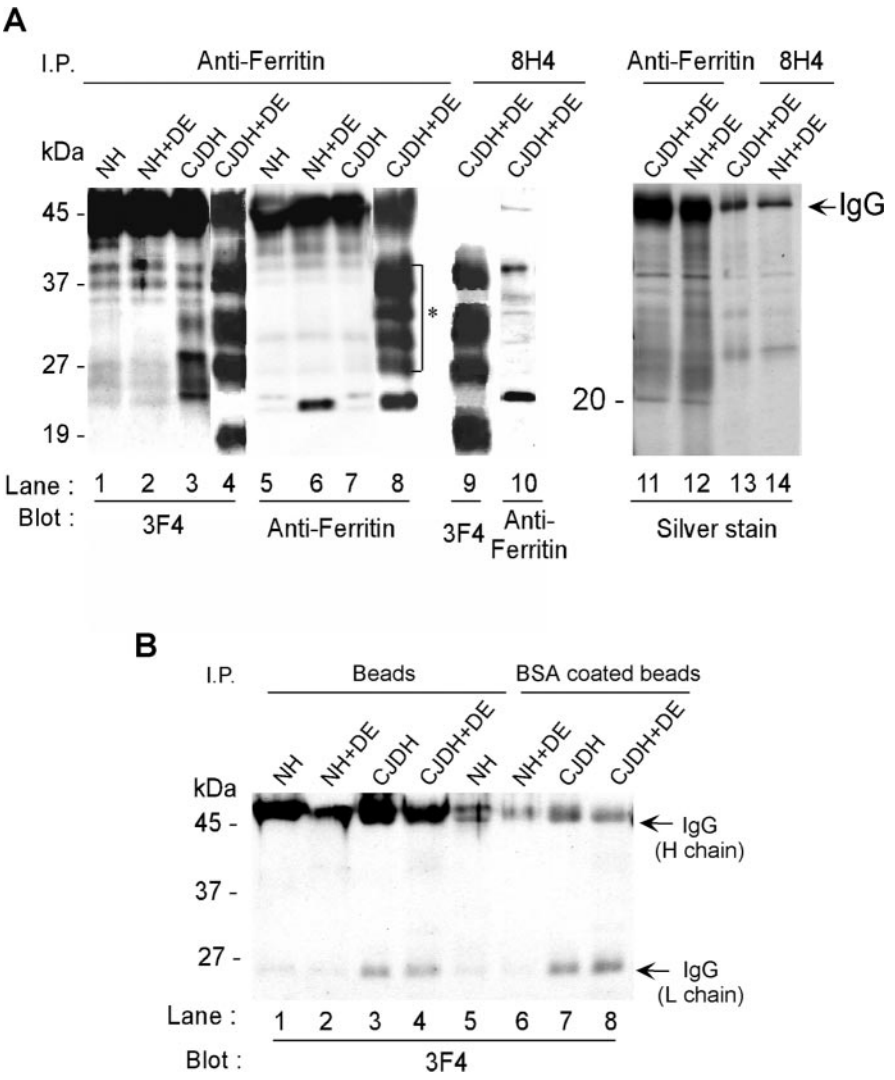


**Figure 5.** The $PrP^{Sc}$–ferritin complex coimmunoprecipitates with anti-ferritin and anti-PrP antibodies. Mock-treated or DE-treated NH and CJDH samples were immunoprecipitated (I.P.) with anti-ferritin or 8H4 antibodies, and coimmunoprecipitated proteins were detected by immunoblotting with specific antibodies. *A*, I.P. with anti-ferritin, followed by probing with 3F4, shows no coimmunoprecipitation of $PrP^{C}$ from NH and NH-DE samples (lanes 1, 2). In contrast, full-length $PrP^{Sc}$ and a significantly greater amount of protease-resistant $PrP^{Sc}$ from CJDH and CJDH-DE immunoprecipitate with anti-ferritin (lanes 3, 4). Reprobing of the same membrane with anti-ferritin shows the H and L chains of ferritin migrating at 21 and 20 kDa in both NH and CJDH samples (lanes 5, 7). The H chain comigrates with the L chain at 20 kDa after DE treatment of NH and CJDH (lanes 6, 8). The identity of additional ferritin-immunoreactive bands in the CJDH-DE sample is unclear (lane 8, *). I.P. of CJDH-DE with 8H4, followed by probing with 3F4, shows $PrP^{Sc}$ bands similar to the ones detected with anti-ferritin I.P. (compare lanes 9, 4). Reprobing with anti-ferritin reveals the 20 kDa ferritin band (lane 10). Silver staining of proteins immunoprecipitated with anti-ferritin or 8H4 shows bands comigrating with ferritin at 20 kDa and several other minor species (lanes 11–14). Note that the IgG band in 8H4 immunoprecipitates is negligible because the antibody was conjugated to protein A beads. A similar conjugation of anti-ferritin reduced the amount of coimmunoprecipitated $PrP^{Sc}$ significantly. *B*, No PrP bands are detected in the absence of primary antibody either with protein A beads or BSA-coated protein A beads (lanes 1–8).

### The binding of sCJD–$PrP^{Sc}$ to Caco-2 cells is partially inhibited by excess ferritin

The persistent association of $PrP^{Sc}$ with ferritin before and after transcytosis led us to investigate whether ferritin acts as a facilitator or a mediator of $PrP^{Sc}$ transport across Caco-2 cells. Accordingly, an attempt was made to competitively inhibit the binding of $PrP^{Sc}$ by preincubating Caco-2 cells with increasing amounts of purified ferritin to saturate available ferritin-binding sites. Two different $PrP^{Sc}$ preparations were used for this purpose: (1) partially denatured biotin-tagged $PrP^{Sc}$ isolated from CJDH that copurifies with ferritin after ultracentrifugation; and (2) biotin-tagged $PrP^{Sc}$–ferritin in its native conformation in CJDH-DE. For competition, three different preparations were used: (1) pure human liver ferritin; (2) pure human spleen ferritin; and (3) brain ferritin purified from NH ($NH^{Pellet}$).

Biotin-tagged $PrP^{Sc}$ was purified by subjecting biotinylated CJDH to PK treatment and repeated rounds of ultracentrifugation, as in Figure 4. A sample from biotinylated NH was subjected to similar treatment, and the resulting pellet fractions from NH ($NH^{Pellet}$) and CJDH ($CJDH^{Pellet}$) were evaluated by Western blotting and silver staining. As expected, immunoblotting with 3F4 shows no reactivity with the NH sample and strong reactivity with N-terminally truncated PK-resistant $PrP^{Sc}$ bands in the CJDH sample (Fig. 8*A*, lanes 1, 2). Reprobing of the membrane with anti-ferritin antibody shows the presence of ferritin in both NH and CJDH samples (Fig. 8*A*, lanes 3, 4). Longer exposure shows the presence of $PrP^{Sc}$ and ferritin oligomers, despite treatment with DTT and boiling in SDS sample buffer (Fig. 8*A*, lanes 5–8, arrows). Silver staining of an aliquot from each sample

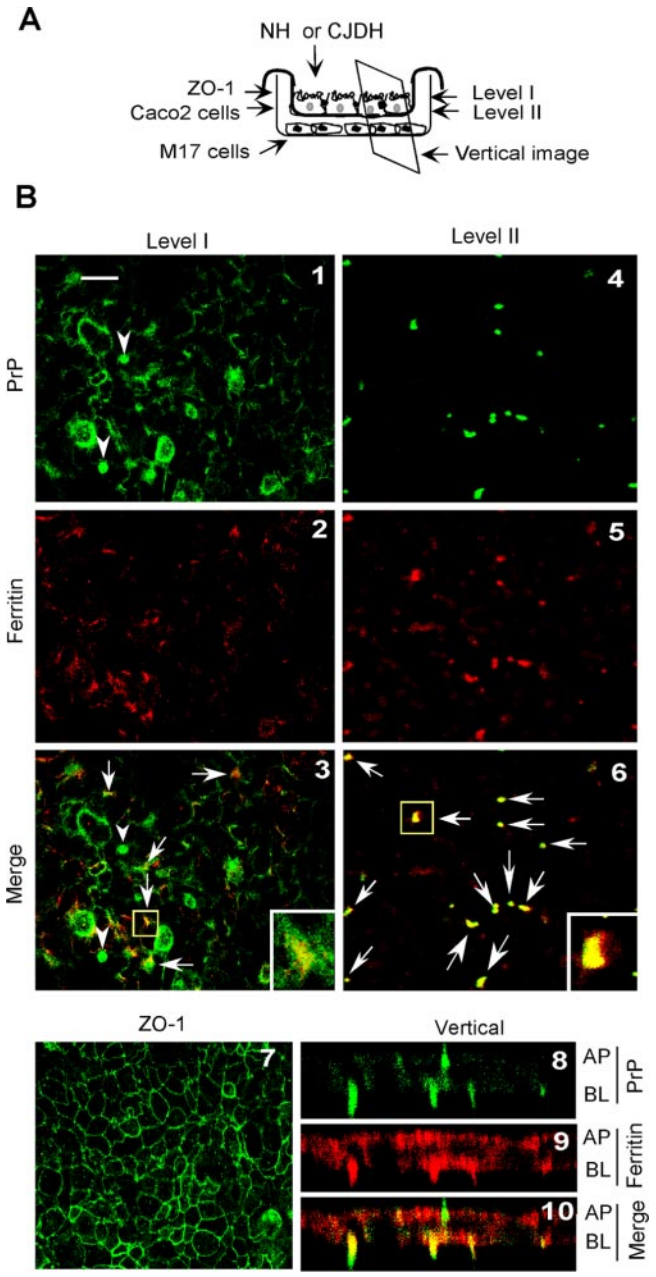


**Figure 6.** sCJD–PrP$^{Sc}$ is cotransported with ferritin across Caco-2 cells. *A*, Diagrammatic representation of filter inserts with Caco-2 cell monolayers and the levels at which images were captured. M17 cells were cultured on glass coverslips in the BL chamber to capture transcytosed PrP$^{Sc}$–ferritin complexes (see Fig. 7*A*). *B*, Caco-2 cell monolayers were incubated with CJDH-DE in the AP chamber for 2 hr, and the filters were cut into two pieces. One was immunostained with 8H4 –anti-mouse FITC (green) and anti-ferritin–anti-rabbit RITC (red) (panels 1–6), and the other was immunostained with with anti-ZO-1–anti-rabbit FITC (green) (panel 7). A horizontal image at level I shows colocalization of PrP (green) and ferritin (red) on the AP surface of Caco-2 cells (panels 1–3, arrows). Some PrP immunoreaction without ferritin is also seen (green) (panels 1–3, arrowheads). A horizontal image captured at level II shows colocalization of PrP (green) and ferritin (red) at the filter pores (panels 4–6, arrows). Immunostaining for ZO-1 shows the presence of tight junctions throughout the monolayer (panel 7). A vertical section through the Caco-2 monolayer shows similar colocalization of PrP (green) and ferritin (red) at the AP and BL membranes, as observed in the horizontal images (panels 8–10). Scale bar: 10 $\mu$m; inset, 2.5×.

showed ferritin in the NH$^{Pellet}$ and ferritin along with PrP$^{Sc}$ in the CJDH$^{Pellet}$ samples, as in Figure 4 (data not shown).

To check whether the purified preparations bind to Caco-2 cells and whether this binding can be competitively inhibited by ferritin, NH$^{Pellet}$ and CJDH$^{Pellet}$ fractions were resuspended in purified human brain lipids lacking all proteins and sonicated to obtain a homogeneous mixture. Subsequently, polarized monolayers of Caco-2 cells were exposed to increasing amounts of NH$^{Pellet}$– and CJDH$^{Pellet}$–brain lipid mixture diluted in PBS containing 1% BSA for 30 min on ice and processed for staining with Texas Red–streptavidin. Remarkably, cells exposed to both NH$^{Pellet}$ and CJDH$^{Pellet}$ show significant binding as determined by biotin-specific reactivity (Fig. 8*B*, panels 1, 2, −Ferritin). Under the experimental conditions used, 16 $\mu$l of NH$^{Pellet}$– and CJDH$^{Pellet}$–brain lipid preparation gave a reproducible and specific signal of defined intensity and was used for competition experiments. Thus, cells were exposed to 0, 0.5, 1.0, and 1.5 $\mu$g/ml human spleen ferritin resuspended in PBS containing 1% BSA for 30 min on ice, washed, and reexposed to 16 $\mu$l of NH$^{Pellet}$ and CJDH$^{Pellet}$ for an additional 30 min on ice. The amount of streptavidin-reactive material bound to Caco-2 cells was determined by staining with Texas Red–streptavidin. Under these experimental conditions, 1.5 $\mu$g/ml pure spleen ferritin inhibits the binding of NH$^{Pellet}$ and CJDH$^{Pellet}$ by ~80%, as determined by comparing the mean fluorescence intensity in 20 different fields (Fig. 8*B*, panels 3, 4, +Ferritin). Anti-ferritin- and PrP-specific antibodies were not used in this experimental setup because immunoreactivity is lost because of DTT treatment. The brain lipid used as vehicle did not show any reaction by itself (data not shown).

The binding of NH$^{Pellet}$ that comprises only human brain ferritin and CJDH$^{Pellet}$ that comprises partially denatured PrP$^{Sc}$ and ferritin and the inhibition of this binding by purified spleen ferritin suggest strongly that the binding of the PrP$^{Sc}$–ferritin complex to Caco-2 cells is mediated by ferritin, not by PrP$^{Sc}$.

Similar competition experiments were performed with biotin-tagged PrP$^{Sc}$ in CJDH-DE, a milieu in which it maintains reactivity to the anti-PrP antibody 8H4. The inhibition of PrP$^{Sc}$ binding in the presence of saturating amounts of ferritin was assessed by double staining with 8H4 and Texas Red–streptavidin. Although significant inhibition (~85%) of PrP$^{Sc}$ binding is observed in the presence of 1.5 $\mu$g/ml spleen ferritin, we did not observe a complete block (Fig. 8*C*, panels 1–6, −Ferritin and +Ferritin). Similar results were obtained when liver ferritin was used as a competitive inhibitor (data not shown).

Our inability to demonstrate >80–85% inhibition of PrP$^{Sc}$ binding despite high concentrations of free ferritin as a competitor led us to conclude that liver and spleen ferritin may not be the optimal inhibitors. Because ferritin in NH$^{Pellet}$ is similar to the ferritin in CJDH-DE in terms of the source and method of preparation, we used NH$^{Pellet}$ to saturate available ferritin-binding sites on Caco-2 cells before adding CJDH-DE. Thus, Caco-2 cells were exposed to 16 $\mu$l of NH$^{Pellet}$–brain lipid suspension for 30 min on ice, washed, and incubated for an additional 30 min on ice with 25 $\mu$l of CJDH-DE. The cells were then immunostained with 8H4 to detect bound PrP$^{Sc}$. Preincubation of the cells with 16 $\mu$l of NH$^{Pellet}$ inhibited the binding of PrP$^{Sc}$ by ~90% (Fig. 8*D*, panels 1, 2, −NH$^{Pellet}$ and +NH$^{Pellet}$).

Together, the above results suggest strongly that ferritin plays a significant role in the binding and transport of the PrP$^{Sc}$–ferritin complex across Caco-2 cells.

## Discussion

This report provides insight into the pathway of PrP$^{Sc}$ uptake and transport across intestinal epithelial cells. In particular, our data show that exposure of sCJD brain homogenate to DEs generates a C-terminal PrP$^{Sc}$ core of 27–30 kDa that is transported across

Caco-2 cells in vesicular structures and that this process is not influenced by the level of endogenous $PrP^C$ expression. Within these vesicles, $PrP^{Sc}$ is associated with ferritin, a major component of the $PrP^{Sc}$–protein complex, and remains associated with ferritin after transcytosis. Because ferritin is normally absorbed from food and is abundantly present in a typical meat dish, these findings have important implications for prion uptake from contaminated food.

Using the well tested *in vitro* model for evaluating intestinal uptake of selected food nutrients (Cereijido et al., 1978; Pinto et al., 1983; Glahn et al., 1998), we show the resilience of $PrP^{Sc}$ to DEs and the facilitative effect of such treatment on $PrP^{Sc}$ uptake by Caco-2 cell monolayers. We noted that after treatment of CJDH with stomach pepsin, $PrP^{Sc}$ underwent limited proteolysis and comigrated with the C-terminal PK-resistant core of $PrP^{Sc}$. Under similar conditions, $PrP^C$ in the NH was completely hydrolyzed. Much to our surprise, DE-treated $PrP^{Sc}$ was transported across Caco-2 cells four times more efficiently than PK-treated $PrP^{Sc}$. We believe that this effect is attributable to the chaotropic effect of bile salts that disperse $PrP^{Sc}$-containing membrane phospholipds into small micelles, preventing the aggregation of $PrP^{Sc}$ and facilitating its binding to epithelial cells. This observation has significant practical implications because there could be qualitative and/or quantitative differences in the digestive process between individuals and certainly between different species. Such differences, although subtle and apparently trivial, may influence host susceptibility to prion infection from contaminated food.

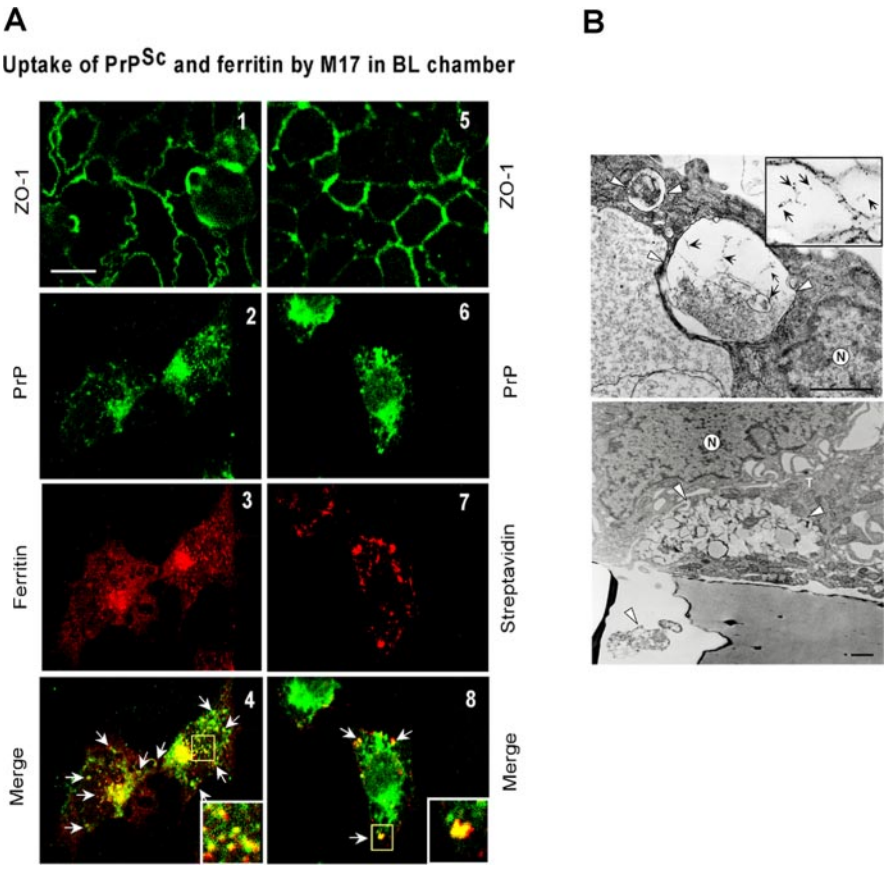


**Figure 7.** sCJD–$PrP^{Sc}$ remains associated with ferritin after transcytosis. *A*, Caco-2 cell monolayers were placed in a 12-well culture dish containing M17 neuroblastoma cells cultured on coverslips in the BL chamber, and biotinylated CJDH-DE was added to the AP chamber (see Fig. 6*A*). After an overnight incubation, Caco-2 cells on filters and M17 cells on coverslips were processed for immunostaining. Immunoreaction of filters with anti-ZO-1 shows the presence of tight junctions in all monolayers (green; panels 1, 5). Immunostaining of M17 cells in the BL chamber for PrP (green) and ferritin (red) shows colocalization of the two proteins, indicating the presence of intact $PrP^{Sc}$–ferritin complexes after transcytosis (panels 2–4, arrows). Coimmunostaining of M17 cells for PrP (green) and streptavidin (red) (panels 6–8) confirms that the PrP signal is derived from biotinylated CJDH-DE in the AP chamber. Scale bar, 10 $\mu$m. *B*, Electron microscopic analysis of the $PrP^{Sc}$–ferritin complex immunoprecipitated with 8H4 shows fibrillar structures and membranes decorated with ferritin aggregates (top inset; arrows). When added to Caco-2 cells, the complex is internalized in relatively large phagosome-like structures surrounded by a single membrane (top; arrowheads). Some of these vesicular structures are extruded out from the BL surface of Caco-2 cells and are seen within the pore of the membrane filter (bottom; arrowhead). (The internalized material in phagosomes shows similar structures as observed in the immunoprecipitated material.) Scale bar: 0.25 $\mu$m; inset, 1.5×. N, Nucleus; T, tight junction.

While purifying $PrP^{Sc}$ from CJDH, we noted that the H and L chains of ferritin consistently cosediment with $PrP^{Sc}$. Resistance of the $PrP^{Sc}$–ferritin complex to elution with low concentrations of salt and coimmunoprecipitation with either anti-PrP or anti-ferritin antibodies suggested an association between the two proteins, rather than coincidental sedimentation. Remarkably, both the H and L chains of ferritin resisted PK and DE treatment and were associated with the protease-resistant core of $PrP^{Sc}$. Electron microscopic examination of the 8H4-immunoprecipitated material revealed fibrils decorated with ferritin aggregates. Although other proteins were detected by silver staining of 8H4 and anti-ferritin immunoprecipitates attesting to the remarkably sticky nature of $PrP^{Sc}$, we believe that the association of $PrP^{Sc}$ with ferritin is stronger and is more likely to be of biological significance. This notion is based on the fact that after repeated rounds of ultracentrifugation, only ferritin remained associated with $PrP^{Sc}$, and the complex could be dissociated only with 0.4 M NaCl. None of the other proteins copurified with $PrP^{Sc}$, suggesting that their coimmunoprecipitation with $PrP^{Sc}$ is perhaps attributable to nonspecific interactions with the antibodies or with $PrP^{Sc}$ itself (N. Morel et al., 2004). Whether the association of $PrP^{Sc}$ and ferritin occurs *in vivo* or after homogenization of brain tissue is unclear from our data. Nevertheless, this complex is biologically significant because ingested $PrP^{Sc}$ in contaminated meat undergoes a process similar to homogenization and DE treatment in the GI tract and is likely presented to the intestinal epithelium in a complex with ferritin. Interestingly, the $\beta$-sheet-rich PrP peptide 106–126 mixed with normal or CJD homogenate was not transcytosed effectively, indicating that the main determinant of $PrP^{Sc}$ transport is not its $\beta$-sheet-rich secondary structure. Preincubation of PrP106–126, NH, or CJDH with exogenous purified ferritin did not facilitate the formation of coimmunoprecipitable PrP–ferritin complexes, indicating that the association of $PrP^{Sc}$ with ferritin is more complex than a mere hydrophobic interaction during the process of homogenization. Regardless of the nature and site of $PrP^{Sc}$–ferritin complex formation, this phenomenon is likely to influence the absorption of ingested $PrP^{Sc}$ significantly, especially because ferritin in ingested food is known to undergo active absorption by the human intestinal epithelium (Murray-Kolb et al., 2003; Theil, 2003).

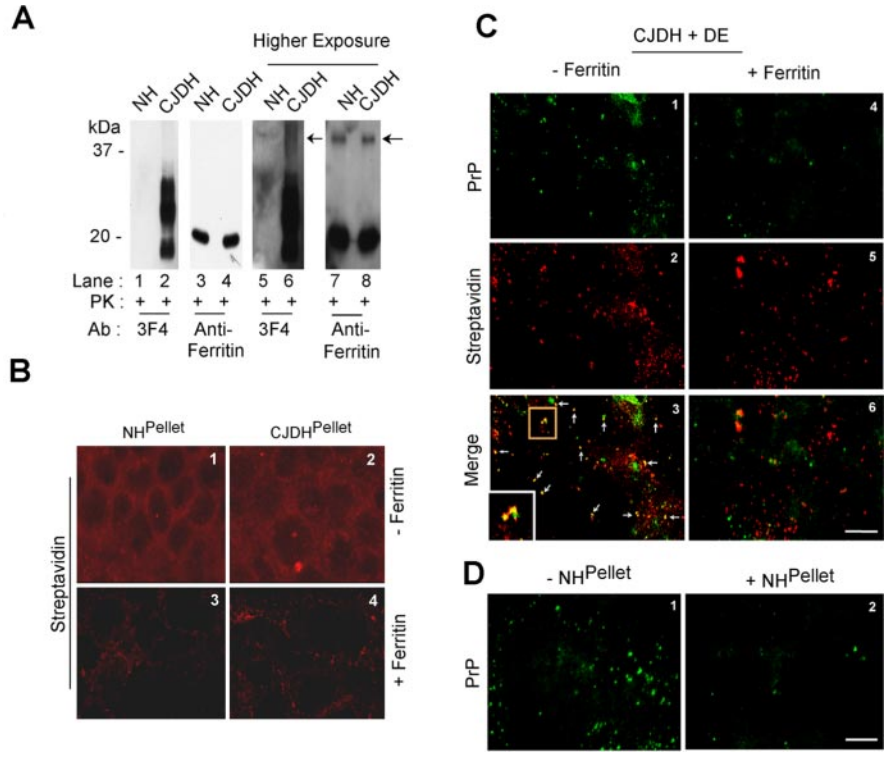


**Figure 8.** The binding of sCJD–PrP$^{Sc}$–ferritin to Caco-2 cells is competitively inhibited by excess ferritin. *A*, Western blotting of NH$^{Pellet}$ and CJDH$^{Pellet}$ fractions with 3F4 reveals no reactivity with the NH sample but strong reactivity with N-terminally truncated PrP$^{Sc}$ bands from the CJDH$^{Pellet}$ sample (lanes 1, 2). Reblotting with anti-ferritin shows the presence of ferritin in both NH and CJDH samples (lanes 3, 4). Longer exposure reveals high molecular weight bands of PrP and ferritin that appear to comigrate (lanes 5–8, arrow). *B*, Caco-2 cell monolayers were incubated with biotin-tagged NH$^{Pellet}$– or CJDH$^{Pellet}$– brain lipid mixture and processed for staining with Texas Red–streptavidin. Both NH$^{Pellet}$ and CJDH$^{Pellet}$ bind to the cell surface (panels 1, 2, −Ferritin), and the binding is inhibited by preincubation of the cells with 1.5 $\mu$g/ml human spleen ferritin (panels 3, 4, +Ferritin). *C*, Caco-2 cells were incubated with 25 $\mu$l of biotinylated CJDH-DE with no previous exposure to ferritin (−Ferritin) or after preincubation with 1.5 $\mu$g/ml human spleen ferritin (+Ferritin) and processed for staining with Texas Red–streptavidin and 8H4–anti-mouse FITC (panels 1–6). Mock-treated cells show PrP-specific immunoreactivity (green) that colocalizes with streptavidin (red) (panels 1–3). However, preincubation with ferritin abolishes PrP-specific staining significantly (panels 4–6). *D*, Caco-2 cells with no previous treatment (panel 1, −NH$^{Pellet}$) or after preincubation with NH$^{Pellet}$– brain lipid mixture containing human brain-derived ferritin (panel 2, +NH$^{Pellet}$) were exposed to 25 $\mu$l of CJDH-DE and immunostained with 8H4–anti-mouse FITC. Mock-treated cells show strong PrP-specific immunoreactivity (panel 1), which is lost significantly after pretreatment of the cells with NH$^{Pellet}$ (panel 2). Scale bar, 10 $\mu$m.

Our data show that 30–40% of ferritin from NH is consistently transcytosed across Caco-2 cells without degradation. In CJDH, this amount varies with the size of PrP$^{Sc}$-ferritin aggregates. Small, detergent soluble complexes are transcytosed intact, whereas large, detergent insoluble aggregates remain on the monolayer in the AP chamber (R. S. Mishra and N. Singh, unpublished observations). These large aggregates may be internalized via M-cells, follicular dendritic cells, or bone marrow-derived dendritic cells as reported previously (Heppner et al., 2001; Huang et al., 2002). It is conceivable that endocytosed ferritin is packaged in distinct vesicles that are either targeted to lysosomes or transcytosed to the BL surface. The associated PrP$^{Sc}$ in CJDH probably follows both routes, although the majority appears to be transcytosed because very little PrP$^{Sc}$ was detected in cell lysates (S. Basu and Singh, unpublished observations). This assumption is supported by the fact that a significant proportion of the PrP$^{Sc}$–ferritin complex remains intact after transcytosis, as evidenced by coimmunostaining of endocytosed aggregates in M17 cells cultured in the BL chamber. PrP$^{C}$ from untreated NH did not show significant association with ferritin and was not transported to the BL chamber in several experiments. However, ferritin from untreated NH was detected consistently in the BL chamber (Basu and Singh, unpublished observations). Thus, either PrP$^{C}$ is not endocytosed at all or is degraded within Caco-2 cells. A small amount of PrP$^{Sc}$ was detected occasionally independent of associated ferritin. It is unclear whether this fraction is associated with another protein, is transported independently, or results from dissociation of the PrP$^{Sc}$–ferritin complex in an intracellular compartment.

Our results show that the PrP$^{Sc}$–ferritin complex is endocytosed by Caco-2 cells in vesicular structures that fuse to form phagosomes within the cell. Some of these vesicles are transcytosed intact to the BL chamber, much like the reported release of PrP$^{Sc}$-containing exosomes into the extracellular environment by epithelial cells (Fevrier et al., 2004). Sensitivity of the PrP$^{Sc}$–ferritin transport to incubation at low temperature and treatment with brefeldin A and nocodazole suggest the involvement of an active transport process (Klausner et al., 1992). Although Caco-2 cells are known to endocytose ferritin, the mechanistic details of this process remain elusive (Murray-Kolb et al., 2003). Specific receptors for ferritin have been reported on liver cells, lymphocytes, erythroblasts, oligodendrocytes, and on various cell lines (Mack et al., 1983; Harrison and Arosio, 1996; Hulet et al., 2000). Our data demonstrating significant inhibition of PrP$^{Sc}$–ferritin uptake in the presence of excess ferritin derived from human liver, spleen, or brain suggests the presence of a ferritin-specific receptor or a transporter on Caco-2 cells. The presence of such a receptor on epithelial cells and the close association of PrP$^{Sc}$ and ferritin in digested food incriminate ferritin as a possible transporter of PrP$^{Sc}$ across the intestinal epithelial cell barrier.

The notion that PrP$^{Sc}$ is cotransported with ferritin ignores the key requirements of host susceptibility to prion infection, such as the level of PrP$^{C}$ expression and the extent of homology between host PrP$^{C}$ and incoming PrP$^{Sc}$ (Prusiner et al., 1990; Weissmann et al., 2002; Thackray et al., 2003). Although in apparent contradiction, our data suggest that the uptake of PrP$^{Sc}$ and its subsequent replication are distinct processes. The former is independent of host PrP$^{C}$, whereas the latter requires PrP$^{C}$ as substrate for additional replication. This hypothesis is supported by our data that show no influence of PrP$^{C}$ overexpression on PrP$^{Sc}$ transport across Caco-2 cells and by a recent report demonstrating PrP$^{C}$ expression below the tight junctions of polarized epithelial cells, making it physically impossible for incoming PrP$^{Sc}$ to come in contact with host PrP$^{C}$ (E. Morel et al., 2004).

The cotransport of PrP$^{Sc}$ with ferritin raises important questions regarding prion uptake from contaminated food. Although this report uses a homologous experimental setup, ferritin H and L chains are known to share significant homology across species (Harrison and Arosio, 1996) and may facilitate the transport of

$PrP^{Sc}$ from distant species across the intestine. Because $PrP^{Sc}$ is notorious for its sticky nature, ferritin may be only one such carrier protein. The identification and functional role of other proteins associated with DE-treated $PrP^{Sc}$ is important for fully understanding the mechanism of $PrP^{Sc}$ uptake from ingested food and preventing a carrier state across species. Heterologous $PrP^{Sc}$ in such carriers may be transported to sites where it may undergo conformational "adaptation" with time (Hill et al., 2000; Race et al., 2001), or in the case of livestock, lie dormant until ingested by a susceptible host. Such apparently "healthy" carriers would disseminate $PrP^{Sc}$ through a variety of means, posing a potential threat to the general population.

## References


Aguzzi A, Polymenidou M (2004) Mammalian prion biology: one century of evolving concepts. Cell 116:313–327.

Baron GS, Caughey B (2003) Effect of glycosylphosphatidylinositol anchor-dependent and -independent prion protein association with model raft membranes on conversion to the protease-resistant isoform. J Biol Chem 278:14883–14892.

Beekes M, McBride PA (2000) Early accumulation of pathological PrP in the enteric nervous system and gut-associated lymphoid tissue of hamsters orally infected with scrapie. Neurosci Lett 278:181–184.

Bons N, Mestre-Frances N, Belli P, Cathala F, Gajdusek DC, Brown P (1999) Natural and experimental oral infection of nonhuman primates by bovine spongiform encephalopathy agents. Proc Natl Acad Sci USA 96:4046–4051.

Cereijido M, Robbins ES, Dolan WJ, Rotunno CA, Sabatini DD (1978) Polarized monolayers formed by epithelial cells on a permeable and translucent support. J Cell Biol 77:853–880.

Collinge J (1999) Variant Creutzfeldt-Jakob disease. Lancet 354:317–323.

Fevrier B, Vilette D, Archer F, Loew D, Faigle W, Vidal M, Laude H, Raposo G (2004) Cells release prions in association with exosomes. Proc Natl Acad Sci USA 101:9683–9688.

Foster JD, Parnham DW, Hunter N, Bruce M (2001) Distribution of the prion protein in sheep terminally affected with BSE following experimental oral transmission. J Gen Virol 82:2319–2326.

Glahn RP, Lee OA, Yeung A, Goldman MI, Miller DD (1998) Caco-2 cell ferritin formation predicts nonradiolabeled food iron availability in an in vitro digestion/Caco-2 cell culture model. J Nutr 128:1555–1561.

Gu Y, Verghese S, Mishra RS, Xu X, Shi Y, Singh N (2003a) Mutant prion protein-mediated aggregation of normal prion protein in the endoplasmic reticulum: implications for prion propagation and neurotoxicity. J Neurochem 84:10–22.

Gu Y, Hinnerwisch J, Fredricks R, Kalepu S, Mishra RS, Singh N (2003b) Identification of cryptic nuclear localization signals in the prion protein: implications for prion disease pathogenesis. Neurobiol Dis 12:133–149.

Haik S, Faucheux BA, Sazdovitch V, Privat N, Kemeny J-L, Perret-Liaudet A, Hauw J-J (2003) The sympathetic nervous system is involved in variant Creutzfeldt-Jakob disease. Nat Med 9:1121–1123.

Harrison PM, Arosio P (1996) The ferritins: molecular properties, iron storage function and cellular regulation. Biochim Biophys Acta 1275:161–203.

Heppner FL, Christ AD, Klein MA, Prinz M, Fried M, Kraehenbuhl J-P, Aguzzi A (2001) Transepithelial prion transport by M cells. Nat Med 7:976–977.

Hill AF, Sidle KC, Joiner S, Keyes P, Martin TC, Dawson M, Collinge J (1998) Molecular screening of sheep for bovine spongiform encephalopathy. Neurosci Lett 255:159–162.

Hill AF, Joiner S, Linehan J, Desbruslais M, Lantos PL, Collinge J (2000) Species-barrier-independent prion replication in apparently resistant species. Proc Natl Acad Sci USA 97:10248–10253.

Huang FP, Farquhar CF, Mabbott NA, Bruce ME, MacPherson GG (2002) Migrating intestinal dendritic cells transport $PrP^{Sc}$ from the gut. J Gen Virol 83:267–271.

Hulet SW, Heyliger SO, Powers S, Connor JR (2000) Oligodendrocyte progenitor cells internalize ferritin via clathrin-dependent receptor mediated endocytosis. J Neuron Res 61:52–60.

Klausner RD, Donaldson JG, Lippincott-Schwartz J (1992) Brefeldin A: insights into the control of membrane traffic and organelle structure. J Cell Biol 116:1071–1080.

Mack U, Powell LW, Halliday JW (1983) Detection and isolation of a hepatic membrane receptor for ferritin. J Biol Chem 258:4672–4675.

McBride PA, Schulz-Schaeffer WJ, Donaldson M, Bruce M, Diringer H, Kretzschmar HA, Beekes M (2001) Early spread of scrapie from the gastrointestinal tract to the central nervous system involves autonomic fibers of the splanchnic and vagus nerves. J Virol 75:9320–9327.

Miller MW, Williams ES (2003) Prion disease: horizontal transmission in mule deer. Nature 425:35.

Mishra RS, Gu Y, Bose S, Verghese S, Kalepu S, Singh N (2002) Cell surface accumulation of a truncated fragment of transmembrane prion protein in GSS P102L. J Biol Chem 277:24554–24561.

Morel E, Fouquet S, Chateau D, Yvernault L, Frobert Y, Pincon-Raymond M, Chambaz J, Pillot T, Rousset M (2004) The cellular prion protein $PrP^{c}$ is expressed in human enterocytes in cell-cell junctional domains. J Biol Chem 279:1499–1505.

Morel N, Simon S, Frobert Y, Volland H, Mourton-Gilles C, Negro A, Sorgato MC, Creminon C, Grassi J (2004) Selective and efficient immunoprecipitation of the disease-associated form of the prion protein can be mediated by nonspecific interactions between monoclonal antibodies and scrapie-associated fibrils. J Biol Chem 279:30143–30149.

Murray-Kolb LE, Welch R, Theil EC, Beard JL (2003) Women with low iron stores absorb iron from soybeans. Am J Clin Nutr 77:180–184.

Nicotera P (2001) A route for prion neuroinvasion. Neuron 31:345–348.

Pan T, Colucci M, Wong BS, Li R, Liu T, Petersen RB, Chen S, Gambetti P, Sy MS (2001) Novel differences between two human prion strains revealed by two-dimensional gel electrophoresis. J Biol Chem 276:37284–37288.

Paramithiotis E, Pinard M, Lawton T, LaBoissiere S, Leathers VL, Zou W-Q, Estey LA, Lamontagne J, Lehto MT, Kondejewski L, Francoeur GP, Papadopoulos M, Haghighat A, Spatz SJ, Head M, Will R, Ironside J, O'Rourke K, Tonelli Q, Ledebur HC, et al. (2003) A prion protein epitope selective for the pathologically misfolded conformation. Nat Med 9:893–899.

Petersen RB, Parchi P, Richardson SL, Urig CB, Gambetti P (1996) Effect of the D178N mutation and codon 129 on the metabolism of the prion protein. J Biol Chem 271:12661–12668.

Peterson MD, Mooseker MS (1992) Characterization of the enterocyte-like brush border cytoskeleton of the C2BBe clones of the human intestinal cell line, Caco-2. J Cell Sci 102:581–600.

Pinto M, Robine-Leon S, Appay M-D, Kedinger M, Triadou N, Haffen K, Fogh J, Zweibaum A (1983) Enterocyte-like differentiation and polarization of the human colon carcinoma cell line Caco-2 in culture. Biol Cell 47:323–330.

Prinz M, Huber G, Macpherson AJS, Heppner FL, Glatzel M, Eugster H-P, Wagner N, Aguzzi A (2003) Oral prion infection requires normal numbers of Peyer's patches but not of enteric lymphocytes. Am J Pathol 162:1103–1111.

Prusiner SB (1998) Prions. Proc Natl Acad Sci USA 95:13363–13383.

Prusiner SB, Scott M, Foster D, Pan KM, Groth D, Mirenda C, Torchia M, Yang SL, Serban D, Carlson GA (1990) Transgenetic studies implicate interactions between homologous PrP isoforms in scrapie prion replication. Cell 63:673–686.

Race R, Raines A, Raymond GJ, Caughey B, Chesebro B (2001) Long-term subclinical carrier state precedes scrapie replication and adaptation in a resistant species: analogies to bovine spongiform encephalopathy and variant Creutzfeldt-Jakob disease in humans. J Virol 75:10106–10112.

Safar J, Wille H, Itri V, Groth D, Serban H, Torchia M, Cohen FE, Prusiner SB (1998) Eight prion strains have $PrP^{Sc}$ molecules with different conformations. Nat Med 4:1157–1165.

Taylor DM (2002) Current perspectives on bovine spongiform encephalopathy and variant Creutzfeldt-Jakob disease. Clin Microbiol Infect 8:332–339.

Thackray AM, Klein MA, Bujdoso R (2003) Subclinical prion disease induced by oral inoculation. J Virol 77:7991–7998.

Theil EC (2003) Ferritin at the crossroads of iron and oxygen metabolism. J Nutr 133:1549S-01553S.

Weissmann C, Enari M, Klöhn P-C, Rossi D, Flechsig E (2002) Transmission of prions. Proc Natl Acad Sci USA 99:16378–16383.